Eur. Phys. J. C 13, 117–123 (2000)
Digital Object Identifier (DOI) 10.1007/s100520000292

THE EUROPEAN PHYSICAL JOURNAL C

The decays $\nu_H \to \nu_L\gamma$ and $\nu_H \to \nu_L e^+e^-$ of massive neutrinos

Q. Ho-Kim[1,a], B. Machet[2,3,b,c], X.Y. Pham[2,3,b,d]

[1] Department of Physics, Université Laval (Québec), Sciences and Engineering Building, Sainte Foy, QC G1K7P4, Canada
[2] Laboratoire de Physique Théorique et Hautes Energies, LPTHE tour 16 / 1^{er} étage, Université P. et M. Curie, BP 126, 4 place Jussieu, 75252 Paris Cedex 05, France
[3] Universités Pierre et Marie Curie (Paris 6) et Denis Diderot (Paris 7), Unité associée au CNRS UMR 7589, Paris, France

Received: 19 August 1999 / Published online: 3 February 2000 – © Springer-Verlag 2000

Abstract. If, as recently reported by the Super-Kamiokande collaboration, the neutrinos are massive, the heaviest one, ν_H, would not be stable and, though chargeless, could in particular decay into a lighter neutrino ν_L and a photon by quantum loop effects. The corresponding rate is computed in the standard model with massive Dirac neutrinos as a function of the neutrino masses and mixing angles. The lifetime of the decaying neutrino is estimated to be $\approx 10^{44}$ years for a mass $\approx 5\times10^{-2}$ eV. Before the mass range arising from present experiments on neutrino oscillations is definitively settled, it is still motivating to study the $\nu_H \to \nu_L e^+e^-$ decay; if kinematically possible, it occurs at tree level and its one-loop radiative corrections get enhanced by a large logarithm of the electron mass acting as an infrared cutoff. Thus the $\nu_H \to \nu_L e^+e^-$ decay largely dominates the $\nu_H \to \nu_L\gamma$ one by several orders of magnitude, corresponding to a lifetime $\approx 10^{-2}$ year for a mass of ≈ 1.1 MeV.

1 The decay $\nu_H \to \nu_L\gamma$

1.1 Introduction

Evidence for the transmutation between the two neutrino species $\nu_\mu \leftrightarrow \nu_\tau$ has recently been reported by the Super-Kamiokande collaboration [1]. As a consequence, neutrinos could have non-degenerate tiny masses, and mixing among different lepton families becomes likely, in analogy with the Cabibbo–Kobayashi–Maskawa flavor mixing in the quark sector [2].

We assume that the neutrino "flavor" eigenstates ν_e, ν_μ and ν_τ are linear combinations of the three-neutrino mass eigenstates ν_1, ν_2 and ν_3 of nonzero and non-degenerate masses m_1, m_2 and m_3 respectively according to

$$\begin{pmatrix}\nu_e\\ \nu_\mu\\ \nu_\tau\end{pmatrix} = \begin{pmatrix}U_{e1} & U_{e2} & U_{e3}\\ U_{\mu1} & U_{\mu2} & U_{\mu3}\\ U_{\tau1} & U_{\tau2} & U_{\tau3}\end{pmatrix}\begin{pmatrix}\nu_1\\ \nu_2\\ \nu_3\end{pmatrix} \equiv \mathscr{U}_{\rm lep}\begin{pmatrix}\nu_1\\ \nu_2\\ \nu_3\end{pmatrix}, \quad (1)$$

where the 3×3 matrix $\mathscr{U}_{\rm lep}$ is unitary.

The effective weak interactions of the leptons can now be written as

$$\mathscr{L}_{\rm eff} = \frac{G_{\rm F}}{\sqrt{2}} L^\dagger_\lambda L^\lambda, \quad (2)$$

where the charged current L_λ is

$$L_\lambda = \sum_\ell \sum_{i=1}^{3} U_{\ell i}\overline{\nu}_i\gamma_\lambda(1-\gamma_5)\ell. \quad (3)$$

Here ℓ stands for e^-, μ^-, τ^-, and ν_i (with $i=1,2,3$) are the three-neutrino mass eigenstates.

Although the neutrinos are chargeless, a heavy neutrino ν_H can decay into a lighter neutrino ν_L by emitting a photon; this decay is entirely due to quantum loop effects.

Neutrino oscillation measurements provide constraints usually plotted in the $(\sin2\theta_{ij}, \Delta m^2_{ij} = |m_i^2 - m_j^2|)$ plane, where θ_{ij} is one of the three Euler angles of the rotation matrix $\mathscr{U}_{\rm lep}$.

For practical purposes, we shall assume for $\mathscr{U}_{\rm lep}$ the following form [3]:

$$\mathscr{U}_{\rm lep} = \begin{pmatrix}\cos\theta_{12} & -\sin\theta_{12} & 0\\ \frac{1}{\sqrt2}\sin\theta_{12} & \frac{1}{\sqrt2}\cos\theta_{12} & -\frac{1}{\sqrt2}\\ \frac{1}{\sqrt2}\sin\theta_{12} & \frac{1}{\sqrt2}\cos\theta_{12} & \frac{1}{\sqrt2}\end{pmatrix}; \quad (4)$$

$\theta_{23} \approx 45^0$ is suggested by the Super-Kamiokande data and $\theta_{13} \approx 0^0$ comes from the CH00Z data [1,3] which give $\theta_{13} \le 13^0$, and also from the Bugey experiment [4], whereas θ_{12} is arbitrary. Although θ_{12} is likely to be small, $\approx 0^0$, the maximal mixing angle $\theta_{12} \approx 45^0$ may also be possible allowing $\nu_e \leftrightarrow \nu_\mu$ (as suggested by the LSND experiment [5,3]).

[a] e-mail: qhokim@phy.ulaval.ca
[b] Member of 'Centre National de la Recherche Scientifique'.
[c] e-mail: machet@lpthe.jussieu.fr
[d] e-mail: pham@lpthe.jussieu.fr

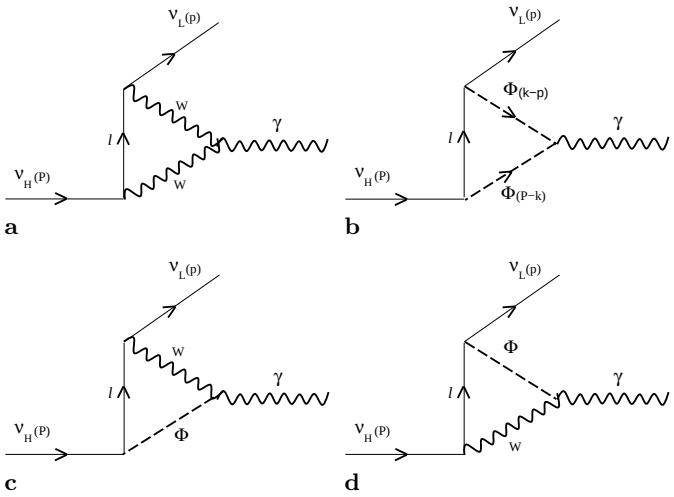

Fig. 1a–d. One-loop diagrams for $\nu_H \to \nu_L\gamma$;

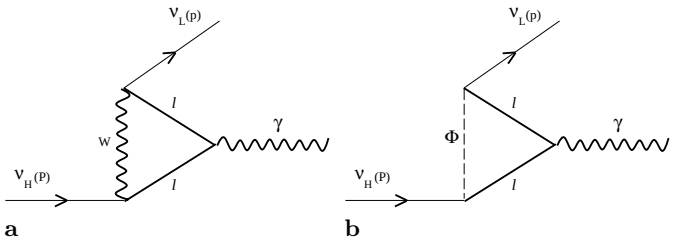

Fig. 2a,b. One-loop diagrams for $\nu_H \to \nu_L\gamma$;

1.2 General considerations

The first calculations of radiative neutrino decays have been reported in [6,7]. Decays of heavy leptons in processes that can violate leptonic numbers have been extensively studied in [8,9]. The reader will find more references in [10].

In the most general renormalizable gauge (conventionally called R_ξ), six Feynman diagrams contribute to the process $\nu_H(P) \to \nu_L(p)\gamma(q)$, where the photon can be real ($q^2 = 0$) or virtual ($q^2 \neq 0$); the latter is necessary when we consider the one-loop radiative corrections to $\nu_H \to \nu_L e^+e^-$. They can be grouped into two sets: four in Figs. 1a–d and two in Figs. 2a–b.

Each one is gauge dependent, but it turns out that the ξ dependence cancels out for each group of diagrams separately, yielding the overall gauge independence of the physical process.

We shall give the results in the 't Hooft–Feynman gauge $\xi = 1$.

For each diagram, the corresponding amplitude $\mathscr{A}$ is written in terms of the effective vertex Γ_μ

$$\mathrm{i}\mathscr{A}_{\nu_H\to\nu_L\gamma} = (-\mathrm{i}e)\left(\frac{\mathrm{i}g}{2\sqrt{2}}\right)^2 \times \sum_\ell U_{L\ell}U^*_{H\ell}\,\overline{u}(p)\Gamma^\mu(\ell)u(P)\varepsilon^*_\mu(q), \quad (5)$$

where the u's are the (Dirac) spinors of the two neutrinos, ε^*_μ is the photon polarization, e the charge of the electron and g the $SU(2)_L$ coupling constant. One has $G_\mathrm{F}/2^{1/2} = g^2/8M_W^2$.

The ultraviolet divergences are handled via the procedure of dimensional regularization, going to $n = 4 - \epsilon$ dimensions.

The mass m of the lightest (outgoing) neutrino is always neglected, such that the results depend on the mass M of the incoming neutrino, the mass M_W of the W gauge boson, and the masses m_ℓ of the internal fermions, which will always appear in the dimensionless ratio

$$r_\ell = \frac{m_\ell^2}{M_W^2}. \quad (6)$$

After expressing the amplitude for each diagram in terms of two-dimensional parametric integrals, we restrict ourselves in this section to the case of a real outgoing photon, for which, due to $q^\mu\varepsilon^*_\mu = 0$ and to the conservation of the electromagnetic current, only the magnetic form factor proportional to $\mathrm{i}\sigma_{\mu\nu}q^\nu$ in the effective vertex contributes (see for example [11,10]). The integration over the Feynman parameters is made simpler by neglecting M^2/M_W^2 in the denominators.

1.3 Explicit computation of the six diagrams

Diagram 1a

The corresponding effective vertex $\Gamma^\mu_{1\mathrm{a}}$ writes

$$\Gamma^\mu_{1\mathrm{a}} = \frac{1}{8\pi^2}(1+\gamma_5)\int_0^1 \mathrm{d}x \int_0^{1-x} \mathrm{d}y \frac{\mathscr{N}^\mu_{1\mathrm{a}}}{\mathscr{D}_1(\ell)} \quad (7)$$

where

$$\mathscr{D}_1(\ell) = M_W^2[(1-x)+r_\ell x] - M^2xy - q^2y(1-x-y) \quad (8)$$

and (γ is the Euler constant $\gamma \approx .577$)

$$\begin{aligned}\mathscr{N}^\mu_{1\mathrm{a}} = \big\{&[2(1-x)(1-y)+y]M^2 \\ &- 2[(1-x)(1-y)+y^2]q^2 \\ &+ 6\mathscr{D}_1(\ell)\left[\frac{2}{\epsilon} + \ln 4\pi - \gamma - \frac{1}{2} - \ln\frac{\mathscr{D}_1(\ell)}{\Lambda^2}\right]\Big\}\gamma^\mu \\ &+ 2M\left\{y(1-2y)P^\mu \right. \\ &\left. + [2y^2 - (1-x)(1+2y)]p^\mu\right\}. \end{aligned} \quad (9)$$

In (9) and in the rest of the paper, Λ is an arbitrary scale coming from the dimensional regularization.

By translational invariance, Γ^μ depends only on the four-momentum transfer q^μ and not on P^μ; the latter may be projected onto the basis formed by three independent four-vectors $\mathrm{i}\sigma^{\mu\nu}q_\nu$, q^μ, and γ^μ, using the following relation valid for $m = 0$:

$$2\overline{u}(p)(1+\gamma_5)P^\mu u(P) = \overline{u}(p)(1+\gamma_5) \times (\mathrm{i}\sigma^{\mu\nu}q_\nu + M\gamma^\mu + q^\mu)\,u(P). \quad (10)$$

This yields

$$\begin{aligned}\mathscr{N}_{1a}^{\mu} &= \mathrm{i}M\sigma^{\mu\nu}q_\nu[x-1-y(1-2x)]\\ &+ \not{q}q^\mu[1-x+3y-2xy-4y^2]\\ &+ \left\{M^2[1-x-2y(1-2x)]\right.\\ &- 2q^2[y^2+(1-x)(1-y)]\\ &+ \left.6\mathscr{D}_1(\ell)\left[\frac{2}{\epsilon}+\ln 4\pi-\gamma-\frac{1}{2}-\ln\frac{\mathscr{D}_1(\ell)}{\Lambda^2}\right]\right\}\gamma^\mu. \quad (11)\end{aligned}$$

The x, y integrations for the pure magnetic term yield the contribution of diagram 1a to the decay amplitude $\nu_H \to \nu_L\gamma$

$$\mathscr{A}_{1a} = \mathscr{A}_0 \sum_\ell U_{H\ell}U_{L\ell}^* F_{1a}(\ell), \quad (12)$$

where

$$\mathscr{A}_0 = \frac{G_F}{\sqrt{2}}\frac{e}{8\pi^2}\overline{u}(p)M(1+\gamma_5)\mathrm{i}\sigma^{\mu\nu}q_\nu u(P)\varepsilon_\mu^*(q). \quad (13)$$

One gets

$$\begin{aligned}F_{1a}(\ell) &= \frac{r_\ell^2(1-3r_\ell)\ln r_\ell}{2(r_\ell-1)^4} \quad (14)\\ &+ r_\ell\left[\frac{7}{12(r_\ell-1)}+\frac{2}{(r_\ell-1)^2}+\frac{1}{(r_\ell-1)^3}\right]-\frac{7}{12}.\end{aligned}$$

The singularities of $F_{1a}(\ell)$ at $r_\ell = 1$ are fake: $F_{1a}(\ell) = -5/12$ for $r_\ell = 1$.

Formula (14) is in agreement with similar calculations [11] for $\mu^- \to e^-\gamma$ in the limit $r_\ell \to 0$, where only the linear term in r_ℓ was kept, and the logarithmic term was neglected.

If m were not neglected, the $M(1+\gamma_5)$ term in (13) would simply be replaced by $M(1+\gamma_5)+m(1-\gamma_5)$. If we keep M^2xy in $\mathscr{D}_1(\ell)$, we will still obtain explicit analytic forms for the Fs but the results will be complicated and not illuminating.

Diagram 1b

Writing in a similar way

$$\Gamma_{1b}^{\mu}(\ell) = \frac{1}{8\pi^2}(1+\gamma_5)\int_0^1 \mathrm{d}x\int_0^{1-x}\mathrm{d}y\frac{\mathscr{N}_b^\mu}{\mathscr{D}_1(\ell)}, \quad (15)$$

one finds

$$\begin{aligned}\mathscr{N}_{1b}^{\mu} &= r_\ell\{M(1-y)[(2y-1)P^\mu\\ &+ (1-2x-2y)p^\mu]\\ &+ \mathscr{D}_1(\ell)\left[\frac{2}{\epsilon}+\ln 4\pi-\gamma-\frac{1}{2}-\ln\frac{\mathscr{D}_1(\ell)}{\Lambda^2}\right]\gamma^\mu\Big\}. \quad (16)\end{aligned}$$

The use of (10) transforms the above expression into

$$\begin{aligned}\mathscr{N}_{1b}^{\mu} &= r_\ell\{\mathrm{i}M\sigma^{\mu\nu}q_\nu x(y-1)\\ &+ \not{q}q^\mu(y-1)(1-x-2y)\\ &+ \big(M^2x(y-1) \quad (17)\\ &+ \mathscr{D}_1(\ell)\left[\frac{2}{\epsilon}+\ln 4\pi-\gamma-\frac{1}{2}-\ln\frac{\mathscr{D}_1(\ell)}{\Lambda^2}\right]\big)\gamma^\mu\Big\},\end{aligned}$$

and, after performing the parametric integration of the purely magnetic term one obtains

$$\begin{aligned}F_{1b}(\ell) &= \frac{r_\ell^2(r_\ell-2)\ln r_\ell}{2(r_\ell-1)^4}\\ &+ r_\ell\left[-\frac{1}{3(r_\ell-1)}-\frac{1}{4(r_\ell-1)^2}+\frac{1}{2(r_\ell-1)^3}\right]. \quad (18)\end{aligned}$$

The singularities of $F_{1b}(\ell)$ at $r_\ell = 1$ are again only apparent; in fact $F_{1b}(\ell) = -1/8$ for $r_\ell = 1$.

The computations proceed along the same way for the other diagrams.

Diagram 1c

$$\begin{aligned}\mathscr{N}_{1c}^{\mu} &= \mathrm{i}M\sigma^{\mu\nu}q_\nu(x+y-1)\\ &+ \not{q}q^\mu(1-x-y)+\left(M^2(x-1)+m_\ell^2\right)\gamma^\mu \quad (19)\end{aligned}$$

gives after the integrations over x and y

$$\begin{aligned}F_{1c}(\ell) &= \frac{-r_\ell^2\ln r_\ell}{2(r_\ell-1)^3}\\ &+ r_\ell\left[\frac{1}{4(r_\ell-1)}+\frac{1}{2(r_\ell-1)^2}\right]-\frac{1}{4}. \quad (20)\end{aligned}$$

Diagram 1d

$$\mathscr{N}_{1d}^{\mu} = m_\ell^2\gamma^\mu \quad (21)$$

yields

$$F_{1d}(\ell) = 0. \quad (22)$$

Diagram 2a

Calling

$$\begin{aligned}\mathscr{D}_2(\ell) &= M_W^2x+m_\ell^2(1-x)\\ &- M^2xy-q^2y(1-x-y) \quad (23)\end{aligned}$$

one has

$$\begin{aligned}\mathscr{N}_{2a}^{\mu} &= 2\mathrm{i}M\sigma^{\mu\nu}q_\nu x(y-1)+2\not{q}q^\mu(1-y)(x+2y)\\ &+\{-2m_\ell^2+2q^2(y-1)(x+y) \quad (24)\\ &- 2\mathscr{D}_2(\ell)\left[\frac{2}{\epsilon}+\ln 4\pi-\gamma-\frac{1}{2}-\ln\frac{\mathscr{D}_2(\ell)}{\Lambda^2}\right]\Big\}\gamma^\mu,\end{aligned}$$

and

$$\begin{aligned}F_{2a}(\ell) &= \frac{r_\ell(2r_\ell-1)\ln r_\ell}{(r_\ell-1)^4} \quad (25)\\ &+ r_\ell\left[\frac{2}{3(r_\ell-1)}-\frac{3}{2(r_\ell-1)^2}-\frac{1}{(r_\ell-1)^3}\right]-\frac{2}{3}.\end{aligned}$$

Diagram 2b

$$\begin{aligned}\mathscr{N}_{2b}^{\mu} &= r_\ell \{iM\sigma^{\mu\nu}q_\nu[x(1+y)-1] \\ &+ \not{q}q^\mu[1-x(1+y)-2y^2] \\ &+ \left(-m_\ell^2 + M^2x + q^2y(x+y-1)\right. \\ &- \left.\mathscr{D}_2(\ell)\left[\frac{2}{\epsilon} + \ln 4\pi - \gamma - \frac{1}{2} - \ln\frac{\mathscr{D}_2(\ell)}{\Lambda^2}\right]\right)\gamma^\mu\Big\}\end{aligned} \tag{26}$$

yields

$$\begin{aligned}F_{2b}(\ell) &= \frac{r_\ell(2-r_\ell)\ln r_\ell}{2(r_\ell-1)^4} \\ &+ r_\ell\left[\frac{-5}{12(r_\ell-1)} + \frac{3}{4(r_\ell-1)^2} - \frac{1}{2(r_\ell-1)^3}\right].\end{aligned} \tag{27}$$

1.4 Cancelation of the ultraviolet divergences

All terms that are ℓ independent do not contribute to the amplitude because of the unitarity of $\mathscr{U}_{\rm lep}$; this is in particular the case of the (divergent) terms $(2/\epsilon + \ln 4\pi - \gamma - 1/2)$ in the diagrams 1a and 2a.

The only two remaining divergent diagrams are 1b and 2b; however the coefficients of their (ℓ-dependent) divergent terms exactly cancel, ensuring the finiteness of the final result.

1.5 Result for the total amplitude of $\nu_H \to \nu_L\gamma$

Dropping the constants $(-7/12), (-1/4), (-2/3)$ in (14), (20) and (25) which, being ℓ independent, do not contribute to the decay amplitude (see above), we obtain for the sum of the six contributions $\sum_\ell U_{H\ell}U^*_{L\ell}[F_{1.a\cdots d}(\ell) + F_{2.a,b}(\ell)]$ the expression

$$\begin{aligned}\mathscr{A}_{\nu_H\to\nu_L\gamma} &= \frac{3}{4}\mathscr{A}_0\sum_\ell U_{H\ell}U^*_{L\ell} \\ &\times \frac{r_\ell}{(1-r_\ell)^3}\left[1 - r_\ell^2 + 2r_\ell\ln r_\ell\right],\end{aligned} \tag{28}$$

where $\mathscr{A}_0$ has been defined in (13). Our result (28) agrees with formula (10.28) for the function $f(r)$ in [10] (where the three irrelevant constants mentioned above are kept).

The corresponding decay rate is

$$\begin{aligned}\Gamma_0 &\equiv \Gamma_{\nu_H\to\nu_L\gamma} \\ &= \frac{G_F^2M^5}{192\pi^3}\left(\frac{27\alpha}{32\pi}\right) \\ &\times \left|\sum_\ell U_{H\ell}U^*_{L\ell}\frac{r_\ell}{(1-r_\ell)^3}\left[1-r_\ell^2+2r_\ell\ln r_\ell\right]\right|^2.\end{aligned} \tag{29}$$

With the assumptions about $\mathscr{U}_{\rm lep}$ and the corresponding mixing angles mentioned in the introduction, one finds for $M \approx 5\times10^{-2}$ eV

$$\Gamma_{\nu_H\to\nu_L\gamma} \approx 10^{-44}/\text{year}. \tag{30}$$

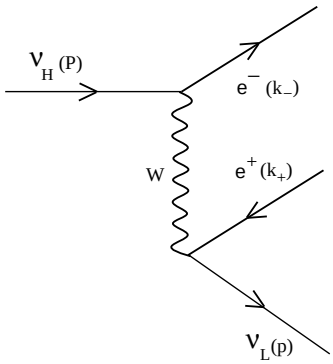

Fig. 3. Tree diagram for $\nu_H \to \nu_L e^+e^-$;

This is to be compared with the experimental lower limit found in [12].

The detectability of this decay and its relevance for astronomy has been emphasized for example in [13].

2 The decay $\nu_H \to \nu_L e^+e^-$

2.1 Generalities

If one believes the combined results on atmospheric and solar neutrinos (see for example [14,15]), there is obviously no space for a "light" non-sterile neutrino with a mass larger than a few 10^{-2} eV; if one includes the LSND results [5], the upper bound can be pushed up to 1 eV, still largely beyond the e^+e^- kinematical threshold.

However, the history of neutrinos has taught us that subtle uncertainties take a long time to be perfectly mastered, and that, in spite of their attractiveness, new and important results must always be confirmed by many different and uncorrelated sources before they are promoted to the status of an unshakable physical reality.

And, still, the present direct experimental limit on the mass of ν_τ is [16] $m_{\nu_\tau} \le 18.2$ MeV. Stronger limits (below 1 MeV) come from cosmological arguments [17,18] but are more likely to be subject to uncertainties.

So, it is still of interest to study the decay $\nu_H \to \nu_L e^+e^-$ (see [10,4] and references therein).

2.2 Computation

If kinematically allowed, this decay is governed at tree level by the diagram of Fig. 3, and at the one-loop level by ten diagrams: the six previously considered in Figs. 1 and 2, where the photon, now off-mass-shell, decays into an electron-positron pair, and the four box diagrams of Fig. 4 in which the $W^+ - W^-$ pair is converted into the $e^+ - e^-$ pair.

The tree amplitude

$$\begin{aligned}\mathscr{A}_{\rm tree} &= \frac{G_F}{\sqrt{2}}U^*_{He}U_{Le}\overline{u}(k_-)\gamma^\mu(1-\gamma_5)u(P) \\ &\times \overline{u}(p)\gamma_\mu(1-\gamma_5)v(k_+)\end{aligned} \tag{31}$$

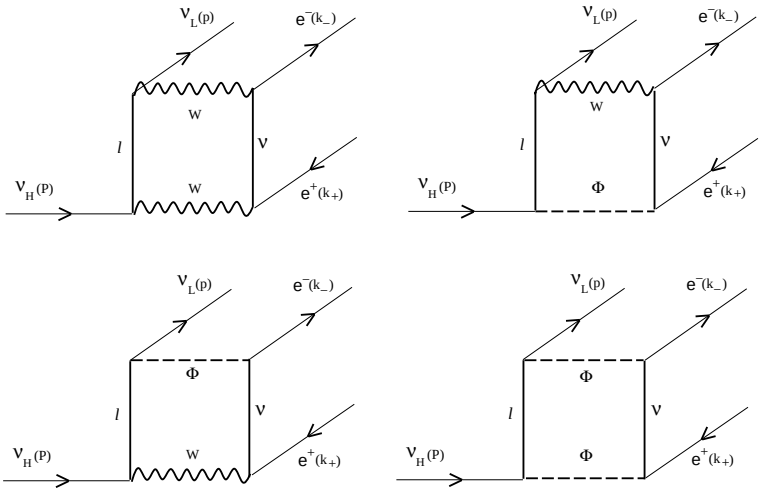

Fig. 4a–d. Box diagrams for $\nu_H \to \nu_L e^+ e^-$;

can be recast, by a Fierz transformation and using the unitarity of $\mathscr{U}_{\rm lep}$, into

$$\mathscr{A}_{\rm tree} = (-1)^2 \frac{G_{\rm F}}{\sqrt{2}} \sum_{j=\mu,\tau} U^*_{Hj} U_{Lj} \overline{u}(p) \gamma^\mu (1-\gamma_5) u(P) \times \overline{u}(k_-) \gamma_\mu (1-\gamma_5) v(k_+). \quad (32)$$

As for the one-loop corrections, a careful examination of all the terms in (11), (17), (19), (21), (24) and (26) for the six vertices $\Gamma^\mu_{1a-d}(\ell), \Gamma^\mu_{2a,b}(\ell)$ shows that the dominant behavior comes from the q^2 term in (24) corresponding to Fig. 2a; it exhibits a contribution $\ln r_\ell \to \infty$ for $r_\ell \to 0$, reflecting mass singularities (or infrared divergences) of the loop integrals.

We can track down this divergent behavior by examining the integration limits $x = 0$ and $x = 1$ of the denominators $\mathscr{D}_{1,2}(\ell)$. When $r_\ell = 0$, an infrared-like divergence occurs if the numerators $\mathscr{N}_2^\mu(\ell)$ lack an x term to cancel the $x = 0$ integration limit of the xM_W^2 term in the denominator $\mathscr{D}_2(\ell)$. This happens with the $2y(y-1)q^2$ term of $\mathscr{N}_{2a}^\mu(\ell)$ in (24).

This infrared-like divergence, which arises when there are two massless ($r_\ell = 0$) internal fermions in the loop, has been noticed a long time ago in the computation of the neutrino charge radius [19].

Compared to $\ln r_\ell$, all other terms are negligible because they are strongly damped by powers of r_ℓ, or $r_\ell^n \ln r_\ell$, where $n > 0$ and $r_\ell < 10^{-3}$. Thus Fig. 2b is damped by $r_\ell \ln r_\ell$, and the four diagrams of Fig. 1 are all strongly damped since an infrared-like divergence cannot occur here: the $x = 1$ integration limit of the $(1-x)M_W^2$ in the denominator $\mathscr{D}_1(\ell)$ is systematically canceled by the $(1-x)$ coming from the integration over the y variable. Explicit x, y integrations of all six vertices $\Gamma^\mu_{1a-d}(\ell), \Gamma^\mu_{2a,b}(\ell)$ confirm these features.

Similar considerations show that the box diagrams of Fig. 4 share the same power suppression $r_\ell^n \ln r_\ell$ as the five other diagrams of Figs. 1a–d and Fig. 2b. The origin of this r_ℓ power suppression in all one-loop diagrams except Fig. 2a can be traced back to the fact that they involve two (W, Φ) propagators; only Fig. 2a and Fig. 2b have one,

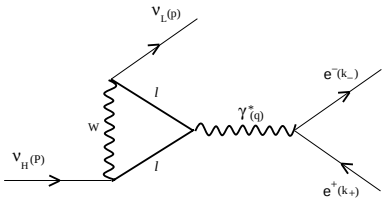

Fig. 5. Leading radiative corrections to $\nu_H \to \nu_L e^+ e^-$

but the latter nevertheless gets an r_ℓ suppression from the Φ fermion couplings.

To summarize, at one loop, only the $2y(y-1)q^2$ term in (24) yields an infrared-like divergence $\propto \ln r_\ell$ while all other terms get damped by powers of r_ℓ.

The leading $q^2 \ln r_\ell$ term of Fig. 2a in the $\nu_H - \nu_L - \gamma$ vertex cancels the photon propagator $1/q^2$ in Fig. 5 and yields an effective local four-fermion coupling proportional to $G_{\rm F}$. The leading contribution to the one-loop radiative corrections to the $\nu_H \to \nu_L e^+ e^-$ tree amplitude is accordingly found to be

$$\mathscr{A}_{rad} = \frac{G_{\rm F}}{\sqrt{2}} \frac{e^2}{24\pi^2} \left[\sum_\ell U^*_{H\ell} U_{L\ell} \ln r_\ell \right] \times \overline{u}(p) \gamma^\mu (1-\gamma_5) u(P) \overline{u}(k_-) \gamma_\mu v(k_+), \quad (33)$$

which can be put, using again the unitarity of $\mathscr{U}_{\rm lep}$ into a form similar to $\mathscr{A}_{\rm tree}$ in (32):

$$\mathscr{A}_{rad} = \frac{G_{\rm F}}{\sqrt{2}} \frac{e^2}{24\pi^2} \left[\sum_{j=\mu,\tau} U^*_{Hj} U_{Lj} \ln \frac{m_j^2}{m_e^2} \right] \times \overline{u}(p) \gamma^\mu (1-\gamma_5) u(P) \overline{u}(k_-) \gamma_\mu v(k_+). \quad (34)$$

The sum $\mathscr{A}_{\rm tree} + \mathscr{A}_{rad} \equiv \mathscr{B}$ is now easy to manipulate when we consider the interference between $\mathscr{A}_{\rm tree}$ and $\mathscr{A}_{rad}$ in $|\mathscr{B}|^2$ for the decay rate.

$$\mathscr{B} = \frac{G_{\rm F}}{\sqrt{2}} \overline{u}(p) \gamma^\mu (1-\gamma_5) u(P) \times \overline{u}(k_-) \gamma_\mu (g_{\rm V} - g_{\rm A} \gamma_5) v(k_+), \quad (35)$$

with

$$g_{\rm V} = \sum_{j=\mu,\tau} U^*_{Hj} U_{Lj} \left(1 + \frac{\alpha}{3\pi} \ln \frac{m_j}{m_e}\right),$$
$$g_{\rm A} = \sum_{j=\mu,\tau} U^*_{Hj} U_{Lj}. \quad (36)$$

From the amplitude $\mathscr{B}$, we compute [20] the decay rate $\Gamma_1 \equiv \Gamma_{\nu_H \to \nu_L e^+ e^-}$ and find

$$\frac{{\rm d}\Gamma_1}{{\rm d}q^2} = \frac{G_{\rm F}^2}{192\pi^3} \frac{\sqrt{q^2(q^2-4m_e^2)}}{q^4 M^3} (M^2-q^2)^2 \times \left\{(g_{\rm V}^2 + g_{\rm A}^2)\left[q^2(M^2+2q^2) + 2m_e^2(M^2-q^2)\right] + 6m_e^2 q^2 (g_{\rm V}^2 - g_{\rm A}^2)\right\}, \quad (37)$$

from which one gets

$$\Gamma_1 = \int_{4m_e^2}^{M^2} {\rm d}q^2 \frac{{\rm d}\Gamma_1}{{\rm d}q^2} = \frac{G_{\rm F}^2 M^5}{192\pi^3} \times \left\{\frac{g_{\rm V}^2 + g_{\rm A}^2}{2} G(x) + (g_{\rm V}^2 - g_{\rm A}^2) H(x)\right\}, \quad (38)$$

where $x = m_e^2/M^2$, and $G(x), H(x)$ are the phase-space functions given by

$$G(x) = \left[1 - 14x - 2x^2 - 12x^3\right]\sqrt{1-4x} + 24x^2(1-x^2) \ln \frac{1+\sqrt{1-4x}}{1-\sqrt{1-4x}}, \quad (39)$$

$$H(x) = 2x(1-x)(1+6x)\sqrt{1-4x} + 12x^2(2x-1-2x^2) \ln \frac{1+\sqrt{1-4x}}{1-\sqrt{1-4x}}. \quad (40)$$

To this leading logarithmic radiative correction expressed by $\approx \alpha \ln r$ in (36) and (38), we may also add the non-leading (simply α, without $\ln r$) electromagnetic correction to the e^+e^- pair. This non-leading correction can be obtained from the one-loop QCD correction to the well known $e^+e^- \to$ quark-pair cross-section, or the $\tau \to \nu_\tau +$ quark-pair decay rate found in the literature [20]; the only necessary change is the substitution $\alpha_s \leftrightarrow 3\alpha/4$. Thus, in addition to Γ_1, we have the non-leading contribution Γ_2

$$\Gamma_2 = \frac{G_{\rm F}^2 M^5}{192\pi^3} \left(\frac{3\alpha}{4\pi}\right) G(x) K(x,x); \quad (41)$$

the function $K(x,x)$ is tabulated in Table 14.1 of [20].

We emphasize that $K(x,x)$ is a spectacular increasing function of x, acting in the opposite direction to the decreasing phase-space function $G(x)$.

If we take, for example, the mass of the heavy decaying neutrino to be 1.1 MeV, its lifetime is found to be $\approx 10^{-2}$ year.

Finally we note that the virtual weak neutral Z^0 boson replacing the virtual photon in Fig. 5 also contributes to $\nu_H \to \nu_L e^+ e^-$. However, it can be safely discarded, being strongly damped by q^2/M_Z^2 due to the Z^0 propagator. Its relevance to the three-neutrinos mode $\nu_H \to \nu_L \nu \bar{\nu}$ may be worth investigating.

3 Conclusion

The recent observation by the Super-Kamiokande collaboration of a clear up–down ν_μ asymmetry in atmospheric neutrinos is strongly suggestive of $\nu_\mu \to \nu_X$ oscillations, where ν_X may be identified with ν_τ or even possibly a sterile neutrino. These results have many important physical implications. In particular, neutrino oscillations mean that neutrinos have a non-vanishing mass, which, according to the new data, may be at least as heavy as 5×10^{-2} eV. If a neutrino ν_H has indeed a mass, it may not be stable against decay and could in principle decay into a lighter neutrino, ν_L, through a cross-family electroweak coupling. We have given here a detailed calculation for the decay modes $\nu_H \to \nu_L \gamma$ which may be also relevant for generalizations to flavor changing processes $Q \to q + \gamma$ in the quark sector.

Waiting for a definitive confirmation of the neutrino mass range coming from oscillation experiments, the present direct upper bounds for there masses do not exclude the decay $\nu_H \to \nu_L e^+ e^-$. In contrast to the former, it arises at tree level and gets further enhanced by large radiative one-loop corrections, is by far the dominant process and may therefore be detectable provided that ν_H has a mass $> 2m_e$. A positive evidence for such decay modes would give a clear signal of the onset of 'new physics'.

Acknowledgements. The work of Q.H.-K. was supported in part by the Natural Sciences and Engineering Research Council of Canada. B.M. and X.Y.P. thank J. Iliopoulos, S. Petcov and F. Vannucci for comments and advice and bringing references to their attention.

References

1. J. Conrad, M. Takita; Talks at the XXIX International Conference on High Energy Physics, Vancouver, Canada July 1998; Y. Fukuda et al., Phys. Rev. Lett. **81**, 1562 (1998)
2. N. Cabibbo, Phys. Rev. Lett. **10**, 531 (1963); M. Kobayashi, T. Maskawa, Prog. Theor. Phys. **49**, 652 (1973)
3. R.D. Peccei: Summary talk at the XXIX International Conference on High Energy Physics, Vancouver (Canada) July 1998
4. C. Hagner et al., Phys. Rev. D **52**, 1343 (1995)
5. C. Athanassopoulos et al., Phys. Rev. Lett. **77**, 3082 (1996); ibid., Phys. Rev. Lett. **81**, 1774 (1998)
6. S.T. Petcov, Yad. Fiz. **25**, 641 (1977) (Sov. J. Nucl. Phys. **25**, 340 (1977); Erratum Sov. J. Nucl. Phys. **25**, 698 (1977)
7. P.B. Pal, L. Wolfenstein, Phys. Rev. D **25**, 766 (1982)
8. B.W. Lee, R.E. Shrock, Phys. Rev. D **16**, 1444 (1977)
9. W.J. Marciano, A.I. Sanda, Phys. Lett. B **67**, 303 (1977)
10. R.N. Mohapatra, P.B. Pal, Massive neutrinos in physics and astrophysics, p. 183 (World Scientific, Singapore 1991)
11. T.P. Cheng, L.F. Li, Gauge theory of elementary particle physics, p. 426 (Oxford University Press, New York 1984)
12. C. Birnbaum et al., Phys. Lett. B **397**, 143 (1997)

13. A. de Rújula, S.L. Glashow, Phys. Rev. Lett. **45**, 942 (1980)
14. S.M. Bilenky, S.T. Petcov, Rev. Mod. Phys. **59**, 671 (1987)
15. S.M. Bilenky, C. Giunti, W. Grimus, Phenomenology of neutrino oscillations, hep-ph/9812360
16. Review of particle properties, Eur. Phys. J. C 3 (1998)
17. A.D. Dolgov, I.Z. Rothstein, Phys. Rev. Lett. **71**, 476 (1993); S. Dodelson, G. Gyuk, M.S. Turner, Phys. Rev. Lett. **72**, 3754 (1994); A.D. Dolgov, S.H. Hansen, D.V. Semikoz, Nucl. Phys. B **524**, 621 (1998); A.D. Dolgov, S.H. Hansen, S. Pastor, D.V. Semikoz, Unstable massive tau-neutrino and primordial nucleosynthesis, hep-ph/9809598 (revised February 1999)
18. P. Fisher, B. Kayser, K.S. McFarland, Neutrino mass and oscillation, hep-ph/9906244 (June 1999)
19. J. Bernstein, T.D. Lee, Phys. Rev. Lett. **11**, 512 (1963); C. Bouchiat, J. Iliopoulos, Ph. Meyer, Phys. Lett. B **42**, 91 (1972)
20. Q. Ho-Kim, X.Y. Pham, Elementary particles and their interactions. Concepts and phenomena (Springer, Berlin, Heidelberg 1998)